Correlation between magnetic softness, sample surface and magnetoimpedance in $Co_{69}Fe_{4.5}X_{1.5}Si_{10}B_{15}$ (X=Ni, Al, Cr) amorphous ribbons

Anurag Chaturvedi [a], Tara Dhakal [a], Sarath Witanachchi [a], Anh-Tuan Le [b], Manh-Huong Phan [a,*], Hariharan Srikanth [a,*]

[a] Department of Physics, University of South Florida, Tampa, FL 33620, USA
[b] Hanoi Advanced School of Science and Technology (HAST), Hanoi University of Technology, 01 Dai Co Viet Street, Hanoi, Viet Nam

ARTICLE INFO

ABSTRACT

The giant magnetoimpedance (GMI) effect and its field sensitivity (η) have been studied in $Co_{69}Fe_{4.5}X_{1.5}Si_{10}B_{15}$ (X=Ni, Al, Cr) amorphous ribbons in the frequency (f) range of 0.1–10 MHz. It is found that at $f < 5$ MHz, the GMI effect and η reach the largest values for the Al-containing sample and the smallest values for the Ni-containing sample, while an opposite trend is observed at $f > 5$ MHz. Magnetization and atomic force microscopy (AFM) experiments reveal that the largest values of the low-frequency GMI effect and η for the Al-containing sample result from the largest value of magnetic permeability, while the largest values of the high-frequency GMI effect and η for the Ni-containing sample are attributed to the smallest surface roughness of this sample. These results point to the importance of the sample surface in determining high-frequency GMI behavior. A correlation between the sample surface and high-frequency GMI is established in the investigated ribbons.

1. Introduction

Soft ferromagnetic amorphous ribbons are widely used for a wide range of applications, including high-frequency transformers and magnetic sensors [1,2]. The recent discovery of a so-called giant magnetoimpedance (GMI) effect in these alloys has made them very attractive candidates for making highly sensitive magnetic sensors [3–8]. The GMI effect is the huge change in the ac impedance (Z) of a ferromagnetic ribbon under the application of a static magnetic field while a high-frequency ac current flows through it [3]. GMI has been explained by means of Maxwell equations solved for certain geometries and particular models [4]. According to this theory, the high-frequency impedance of a ferromagnetic ribbon can be calculated by

$$Z = R_{dc} jka \coth(jka), \tag{1}$$

where a is half of the thickness of the ribbon, R_{dc} is the electrical resistance for a dc current, j is the imaginary unit, and $k = (1+j)/\delta_m$. The penetration depth or skin depth (δ_m) in a magnetic medium, with the transverse permeability (μ_T) is given by

$$\delta_m = (\rho/\pi\mu_T f)^{1/2}, \tag{2}$$

where ρ is the electrical resistivity, μ_T is the transverse magnetic permeability, and f is the frequency of the ac current. In non-magnetic materials, δ_m can be controlled by changing the frequency. In magnetic materials, the application of a magnetic field changes μ_T, δ_m, and consequently Z. According to Eqs. (1) and (2), GMI effect should be expected in ferromagnetic ribbons with large μ_T and small δ_m and small R_{dc} [4]. However, this condition is valid for the low-frequency regime and may become different for the high-frequency regime when the skin effect is strong and the effect of sample surface is significant [9–13].

To further elucidate this, we have studied systematically the influences of magnetic softness and sample surface on the GMI behavior in $Co_{69}Fe_{4.5}X_{1.5}Si_{10}B_{15}$ (X=Ni, Al, Cr) amorphous ribbons in the frequency range of 0.1–10 MHz. The results obtained reveal that the largest values of the GMI effect and the field sensitivity of GMI for the Al-containing sample for $f < 5$ MHz result from the largest value of saturation magnetization (M_S) determined from the magnetization loop. However, the largest values of the GMI effect and the field sensitivity of GMI for the Ni-containing sample for $f > 5$ MHz are attributed to the smallest surface roughness of this sample. These results point to the importance of the sample surface in determining high-frequency GMI behavior.

2. Experimental

$Co_{69}Fe_{4.5}X_{1.5}Si_{10}B_{15}$ (X=Ni, Al, Cr) amorphous ribbons with a width of 1 mm and a thickness of 16 μm were prepared by the melt-spinning method. X-ray diffraction confirmed the amorphous nature of the alloys and the atomic percentages of the

* Corresponding authors. Tel.: +1 813 9744714.
E-mail addresses: tuanla-hast@mail.hut.edu.vn (A.-T. Le), mphan@cas.usf.edu (M.-H. Phan), sharihar@cas.usf.edu (H. Srikanth).

elements were established by inductive coupled plasma spectroscopy [14]. The ribbon samples of 5 mm length were used for the present study. The surface morphology of the samples was analyzed using atomic force microscopy (AFM). Field dependent magnetization (*M–H*) measurements were performed at room temperature using a Physical Property Measurement System (PPMS) from Quantum Design. Magnetoimpedance measurements were carried out along the ribbon axis in applied dc magnetic fields up to 120 Oe over a frequency range of 0.1–10 MHz with the ac current directed along the ribbon axis. An impedance analyzer (HP4192A) was used in the four-terminal contact mode to measure the absolute value of the impedance of the sample at room temperature. The detail of the magnetoimpedance measurement system has been reported elsewhere [15].

From the measured impedance, the percentage change of magnetoimpedance (i.e., the GMI ratio) with applied magnetic field is expressed as

$$\Delta Z/Z(\%) = 100\% \times [Z(H) - Z(H_{max})]/Z(H_{max}) \tag{3}$$

and the dc magnetic field sensitivity of GMI as

$$\eta = 2 \times \frac{[\Delta Z/Z(\%)]_{max}}{\Delta H}, \tag{4}$$

where H_{max} is the maximum applied dc magnetic field to saturate the impedance of the ribbon. ΔH is a measure of the full-width at half-maximum (FWHM) of the ($\Delta Z/Z$)% vs. *H*.

3. Results and discussion

Fig. 1 shows the AFM images of the surface topography of the $Co_{69}Fe_{4.5}X_{1.5}Si_{10}B_{15}$ (X=Ni, Al, Cr) amorphous ribbon samples. The AFM images clearly indicate the distribution of protrusions with very high and uniform density for the Ni- and Al-containing samples, but not for the Cr-containing sample. From the corresponding topographical data of Fig. 1, the root-mean-squared (rms) surface roughness ($R_q = 1/n^2 \sqrt{\sum_{i=1}^{n} z_i^2}$, where *z* is the average amplitude of the topographical feature) was determined to be about 2.153 nm for the Ni-containing sample, 3.098 nm for the Al-containing sample and 5.673 nm for the Cr-containing sample.

Fig. 2 shows *M–H* loops taken at room temperature for $Co_{69}Fe_{4.5}X_{1.5}Si_{10}B_{15}$ (X=Ni, Al, Cr) amorphous ribbons. It can be observed that the saturation magnetization (M_S) and magnetic permeability (μ) are largest for the Al-containing sample and smallest for the Ni-containing sample. Meanwhile, the coercivity (H_c) is almost the same for all the samples.

Fig. 3 shows the magnetic field dependence of GMI ratio ($\Delta Z/Z$) at frequencies, *f*=1 and 6 MHz, for the $Co_{69}Fe_{4.5}X_{1.5}Si_{10}B_{15}$ (X=Ni, Al, Cr) amorphous ribbon samples. As one can see clearly from Fig. 3a, for the case at 1 MHz, $\Delta Z/Z$ reaches the largest value for the Al-containing sample and the smallest value for the Ni-containing sample, whereas the sample with Ni has the highest $\Delta Z/Z$ for the case at 6 MHz (Fig. 3b). The sample with Cr has the lowest GMI ratio at *f*=6 MHz.

To better illustrate this feature, we display in Fig. 4a, b the frequency dependence of maximum GMI ratio ($[\Delta Z/Z]_{max}$) and the field sensitivity of GMI (η) for all samples investigated. A general trend observed for all the samples is that with increasing frequency in the range of 0.1–10 MHz, $[\Delta Z/Z]_{max}$ first increases, reaches a maximum at a critical frequency (f_0), and then decreases for higher frequencies. This trend can be interpreted by considering the relative contributions of domain wall motion and magnetization rotation to the transverse permeability and hence the GMI effect [4]. At frequencies below 1 MHz ($a < \delta_m$), $[\Delta Z/Z]_{max}$ is relatively low due to the contribution of the induced magneto-inductive voltage to the measured magnetoimpedance [3]. In the range
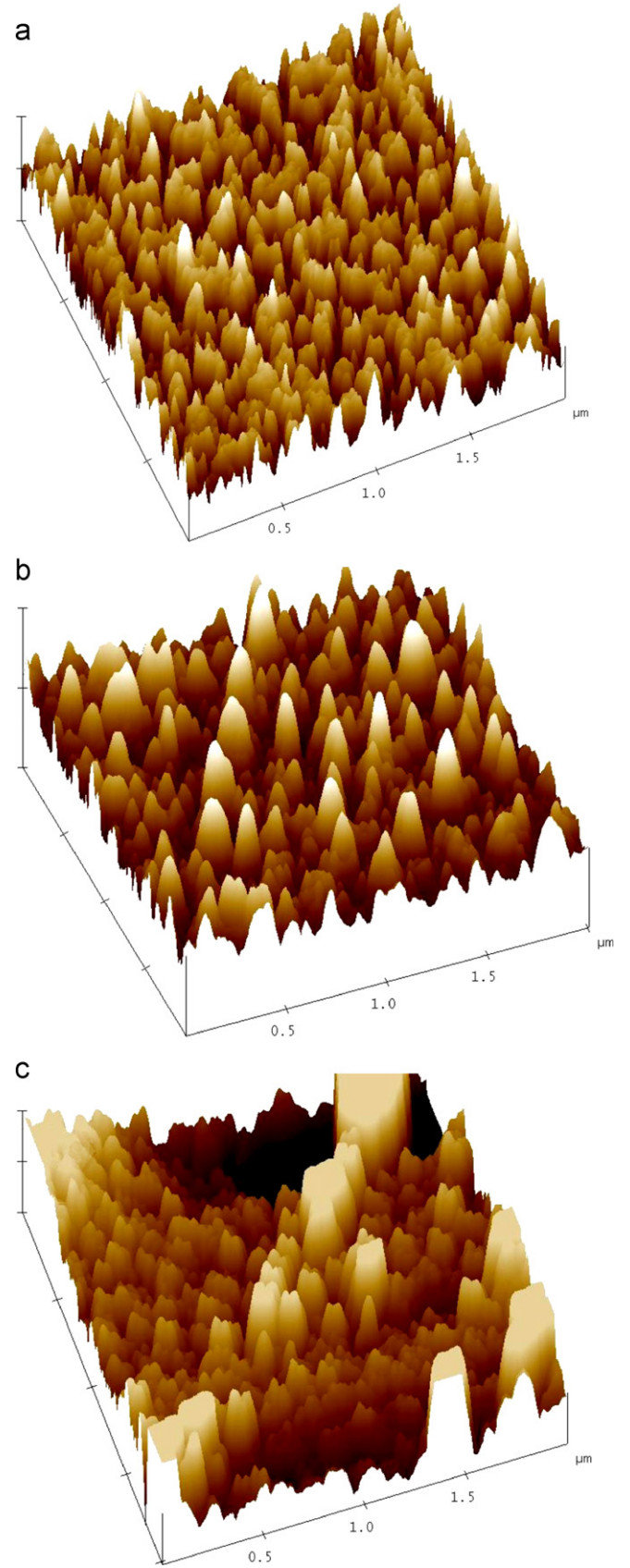

Fig. 1. 3-D AFM images of (a) the $Co_{69}Fe_{4.5}Ni_{1.5}Si_{10}B_{15}$ amorphous ribbon, (b) the $Co_{69}Fe_{4.5}Al_{1.5}Si_{10}B_{15}$ amorphous ribbon, and (c) the $Co_{69}Fe_{4.5}Cr_{1.5}Si_{10}B_{15}$ amorphous ribbon.